Results from the BRAHMS experiment at RHIC

Dieter Röhrich
for the BRAHMS Collaboration:
I. G. Bearden[8], D. Beavis[1], C. Besliu[11], Y. Blyakhman[7], J. Brzychczyk[4], B. Budick[7], H. Bøggild[8], C. Chasman[1], C. H. Christensen[8], P. Christiansen[8], J. Cibor[5], R. Debbe[1], J. J. Gaardhøje[8], M. Germinario[8], K. Grotowski[4], K. Hagel[9], O. Hansen[8], A. Holm[8], A. K. Holme[2], H. Ito[1], E. Jakobsen[8], A. Jipa[11], J. I. Jordre[10], F. Jundt[3], C. E. Jørgensen[8], T. Keutgen[9], E. J. Kim[6], T. Kozik[4], T. M. Larsen[2], J. H. Lee[1], Y. K. Lee[6], G. Løvhøiden[2], Z. Majka[4], A. Makeev[9], B. McBreen[1], M. Murray[9], J. Natowitz[9], B. S. Nielsen[8], K. Olchanski[1], J. Olness[1], D. Ouerdane[8], R. Płaneta[4], F. Rami[3], D. Roehrich[10], B. Samset[2], D. Sandberg[8], S. Sanders[12], R. A. Sheetz[1], Z. Sosin[4], P. Staszel[8], T. F. Thorsteinsen[10+], T. S. Tveter[2], F. Videbæk[1], R. Wada[9], A. Wieloch[4], and I. S. Zgura[11]
[1] Brookhaven National Laboratory, Upton, USA
[2] Fysisk Institutt, University of Oslo, Blindern, Norway
[3] IReS, University Louis Pasteur, Strasbourg, France
[4] Jagiellonian University, Krakow, Poland
[5] Institute of Nuclear Physics, Krakow, Poland
[6] Johns Hopkins University, Baltimore, USA
[7] New York University, New York, USA
[8] Niels Bohr Institute, University of Copenhagen, Denmark
[9] Texas A&M University, College Station, USA
[10] University of Bergen, Norway
[11] University of Bucharest, Romania
[12] University of Kansas, USA
[+] *Deceased*

Department of Physics, University of Bergen, Allegaten 55, 5007 Bergen, Norway.

Abstract. Results from the BRAHMS collaboration for the inaugural physics running with the Relativistic Heavy Ion Collider (RHIC), Au+Au collisions at $\sqrt{s_{NN}} = 130$ GeV in the late summer of 2000, and some results of the very first data from the summer of 2001 at $\sqrt{s_{NN}} = 200$ GeV are presented. The main focus is here on the determination of the pseudorapidity distribution of charged particles as a function of collision centrality and on the measurement of the antiproton to proton and the K$^-$ to K$^+$ ratio as a function of rapidity. The pseudorapidity density at midrapidity reaches $dN(ch)/d\eta = 553 \pm 36$ for the most central collisions (0-5%) at $\sqrt{s_{NN}} = 130 GeV$; the corresponding number for the higher energy is $dN(ch)/d\eta = 632 \pm 36$, demonstrating an increase in multiplicity of about 14%. The measured antiproton/proton ratios peak at midrapidity around $N(\bar{p})/N(p) = 0.64 \pm 0.06$ and drop to 0.41 ± 0.04 at $y \approx 2$ for $\sqrt{s_{NN}} = 130$ GeV reactions; the K$^-$ to K$^+$ ratios are 0.90 ± 0.06 ($y \approx 0$) and 0.83 ± 0.1 ($y \approx 2.5$).

1. Introduction

In late August 2000 the Relativistic Heavy Ion Collider at Brookhaven National Laboratory, NY, USA, began colliding Au beams, each at an energy of $65AGeV$, with sufficient duty cycle and luminosity to permit the beginning of systematic data collection by the four RHIC experiments. In mid-August 2001, systematic data taking at $100AGeV + 100AGeV$ began. Results from the analysis of the first data taken with the BRAHMS (Broad Range Hadronic Magnetic Spectrometer) detector are going to be reported.

2. The BRAHMS experiment

Fig. 1 shows a schematic picture of the layout of the BRAHMS experiment. The BRAHMS detector system [1] consists of two independent magnetic spectrometers that can be positioned over an angular range from 2.3° to 30° (forward spectrometer, FS) and from 30° to 90° (midrapidity spectrometer, MRS) with respect to the beam line. The spectrometers are used to fully identify charged particle over a large range in rapidity y, and transverse momentum p_t (see fig. 2, left panel). Fig. 1 (right panel) shows the full acceptance of BRAHMS. Due to the small solid angle of each spectrometer (6 msr and 0.5 msr, respectively) the acceptance must be explored through numerous combinations of angular and field settings. In the initial runs of 2000 the backend of the FS was not used. In the 2001 runs the full FS was operational and has already shown to provide excellent particle identification to $p < 25$ GeV/c.

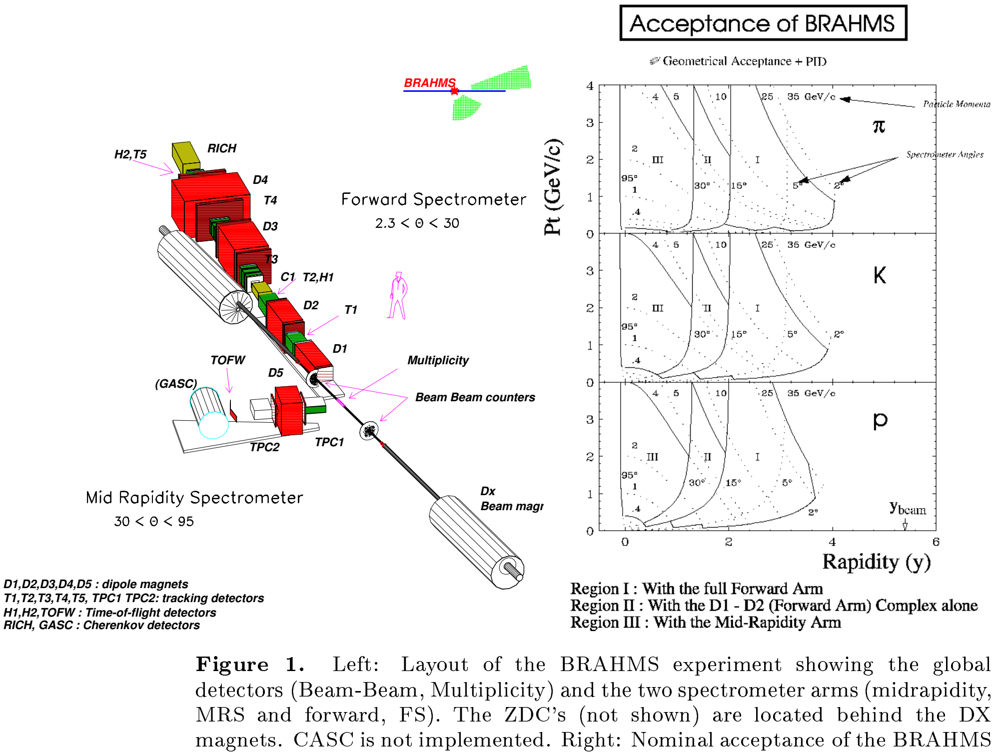

Figure 1. Left: Layout of the BRAHMS experiment showing the global detectors (Beam-Beam, Multiplicity) and the two spectrometer arms (midrapidity, MRS and forward, FS). The ZDC's (not shown) are located behind the DX magnets. CASC is not implemented. Right: Nominal acceptance of the BRAHMS spectrometers for identified hadrons.

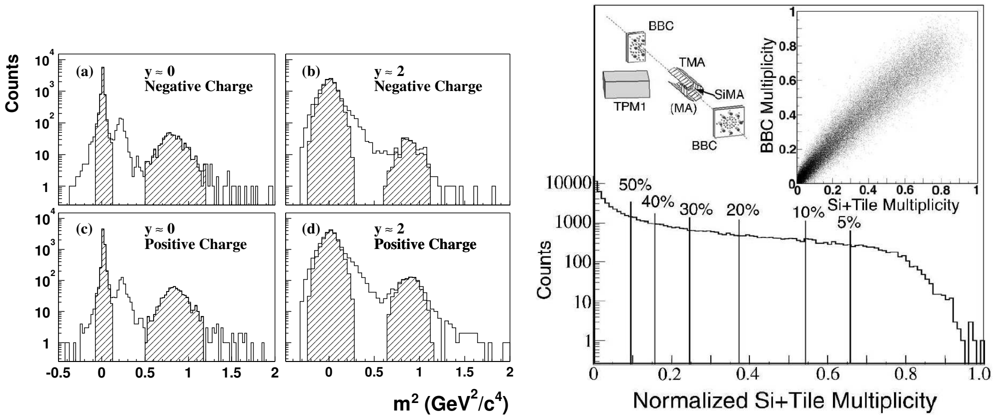

Figure 2. Left panel: m^2 distributions for charged particles identified in the BRAHMS spectrometers. Left panels show data for the MRS positioned at 90° with respect to the beam direction, right panels show data from the FS at 4° ($y = 2$). The upper and lower rows are for negative and positive particles respectively. The shaded regions show the pions and protons selected for the analysis on the basis of fiducial cuts on time–of–flight. Right panel: Normalized multiplicity distribution of charged particles obtained using the SiMA and TMA for Au+Au collisions at $\sqrt{s_{NN}} = 130$ GeV. The insert shows the good correlation between the multiplicities deduced from the signals in these two detectors.

The BRAHMS experiment has four different global detector systems. The Beam-Beam Counters (BB) consist of two arrays of a total of 79 Lucite Cerenkov radiators coupled to phototubes positioned ± 2.15 m from the nominal intersection point and measure charged hadrons in the pseudo-rapidity range of $2.1 < |\eta| < 4.7$. The Zero Degree Calorimeters (ZDC) [2] at ±18 m measure non-interacting neutrons from the collisions. The time difference between the two ZDC signals allows a determination of the collision vertex with a precision of ≈ 2.5 cm. A scintillator tile multiplicity array (TMA) measures charged particle emission in the central pseudorapidity region ($-2.0 < \eta < +2.0$) and is used for centrality selection and determination of the multiplicity of charged particles as a function of pseudorapidity. A silicon multiplicity array (SiMA) ($-2.2 < \eta < +2.2$) provides additional information on charged particle multiplicity in the central region. The SiMA is configured as a tube of hexagonal cross section placed inside the TMA. Each side, or ladder, consists of 8 Si detectors ($300\mu m$ thick). Due to the spread in collision vertices these two arrays provide charged particle multiplicity information in the range $-3 < \eta < +3$ (see fig. 2, right panel). Combined with the beam-beam information the three arrays cover the range $-4.7 < \eta < +4.7$.

3. Antiproton to proton ratios vs rapidity - stopping

Stopping is a measure of the conversion of the incoming longitudinal energy of a projectile and target into transverse degrees of freedom, hence the slowing down of incoming nucleons. Stopping is typically studied by assessing the average rapidity loss $\langle \delta y \rangle = y_p - \langle y_b \rangle$, where y_p is the incoming projectile rapidity and $\langle y_b \rangle$ is the average net baryon rapidity after the collision. Fig. 3 (middle panel) shows the rapidity distributions of net protons in central Pb+Pb collisions at 158 GeV/nucl. (Experiment NA49 at SPS [17]). In going from peripheral to central collisions, the rapidity at which the largest yield is observed moves toward mid-rapidity, indicating a significant increase in stopping. A similar behaviour is observed at AGS energies [18].

The mean rapidity shift of protons scaled to the beam rapidity as function of the bombarding energy is shown in the left panel of fig. 3 [19, 20]. The average rapidity loss scales with the beam rapidity in the regime from 1 to 200 AGeV. For the heavier systems the relative rapidity loss is 32%. Assuming that this value is true for RHIC energies, one would expect a rapidity density of net protons at midrapidity of about 10-15 what is consistent with measurements at $\sqrt{s_{NN}} = 130$ GeV [21, 22, 23] (see fig. 3, right panel).

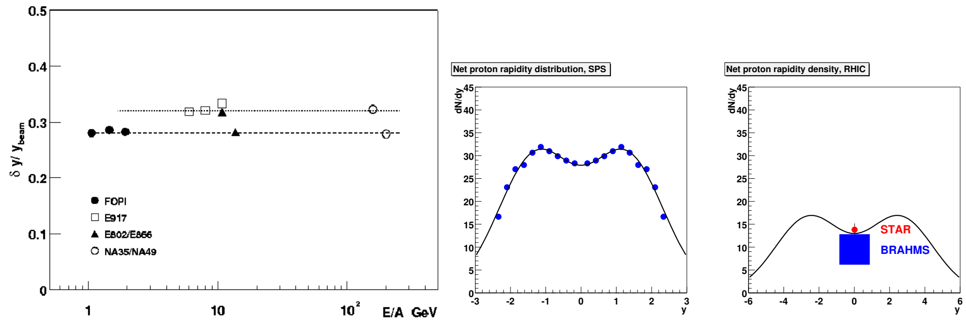

Figure 3. Left panel: Mean rapidity shift of protons scaled to the beam rapidity as function of the bombarding energy (see [20] and references therein). Middle panel: Rapidity distributions of net protons for central Pb+Pb collisions at 158 GeV/nucl. (Experiment NA49 at SPS [17]). A double Gaussian fit is also shown. Right panel: Extrapolated rapidity distribution net protons for central Au+Au collisions at RHIC. Preliminary results are also shown [21, 22, 23].

Due to the ability to identify particles over a broad range in rapidity, BRAHMS is well suited to study the mechanism underlying the stopping of the baryons of the colliding nuclei. Fig. 4 shows the first measurements [5] of the $N(\bar{p})/N(p)$ ratio at rapidities around $y = 0, 0.7$ and 2 together with similar $N(\pi^-)/N(\pi^+)$ ratios at $y \approx 0, 1$ and 3 for $\sqrt{s_{NN}} = 130$ GeV collisions. While the meson ratios are close to unity, the measured antiproton to proton ratios vary from about 64% at $y = 0$, to 66% at $y = 0.7$ and 41% at $y = 2$ for 0-40% collision centrality. The results show that a net-baryon free midrapidity region has not been attained, although the $N(\bar{p})/N(p)$ ratio is the highest that has been measured so far in nucleus-nucleus collisions. The STAR collaboration has measured similar particle ratios at $y = 0$ in a narrower momentum range [21] and their results agree well with the $y = 0$ measurements presented here.

Fig. 4 shows $N(\bar{p})/N(p)$ as a function of rapidity at SPS [17, 24]. At SPS the distribution is sharply peaked at midrapidity, while at RHIC the data indicate that the ratio is constant over $\pm$ 0.7 units of rapidity. The $N(\bar{p})/N(p)$ ratio of 0.64 (RHIC) at $y = 0$ is considerably higher than similar ratios measured in Pb+Pb collisions at SPS ($\approx 0.07 - 0.15$ at $\sqrt{s_{NN}}$=17 GeV) [11, 17] and at AGS ($\approx 2.5 \cdot 10^{-4}$ at $\sqrt{s_{NN}} = 5$ GeV) [10].

Fig. 4 also compares the measured ratios to model calculations [12, 13, 14] using the same cuts on centrality and transverse momentum as those applied in the data analysis. All three models reproduce the observed pion ratios well. The FRITIOF model reproduces the antiproton/proton ratios quite well, but it overpredicts the charged particle yield at $\eta \approx 0$ by $\approx 30\%$ [3]. On the other hand the HIJING model which describes the overall charged particle yields well, fails in describing the

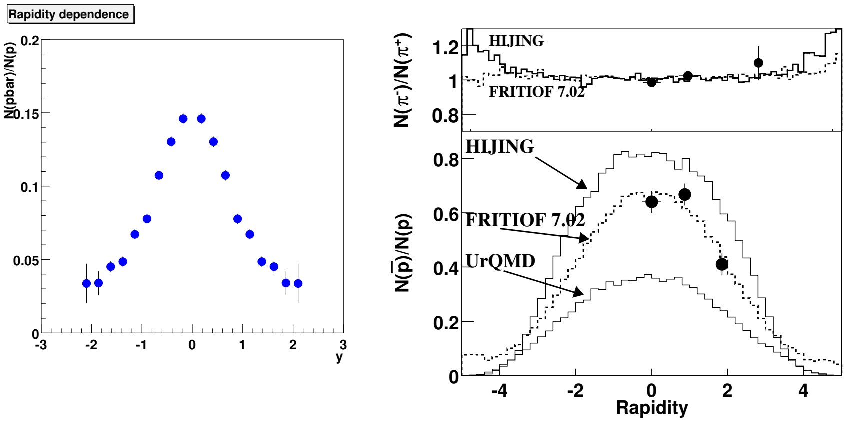

Figure 4. The figures show the rapidity dependence of the $N(\bar{p})/N(p)$ ratio at SPS (left panel) and RHIC (right panel). Also shown (right panel) is a comparison of the measured $N(\bar{p})/N(p)$ (lower band) and $N(\pi-)/N(\pi^+)$ (upper band) ratios to model predictions (HIJING, FRITIOF, UrQMD). The data shown are for 0-14% (SPS) and 0-40% (RHIC) central events.

anti-proton to proton ratios. The UrQMD transport model underpredicts the ratio by almost a factor of about two and overpredicts the total charged particle multiplicity.

4. Pseudorapidity densities of charged particles

As described above, the charged particle multiplicity can be determined by measuring the total energy deposited in a BB, SiMA or TMA detector element and dividing by the average energy deposited by charged particles in that detector element [3]. The identification of the collision vertex is crucial for the assignment of particles to the pseudorapidity bins and for calculations of energy loss. Likewise, the measurements involve important corrections for the inevitable production of secondary charged particles resulting from interactions in the beam pipe and in other material around the detectors. These contributions have been estimated in GEANT simulations of the experiment using various event generators as input. The correction factors vary for the various detector systems and range from about 37% at $\eta = 0$ to about 50% at $\eta = 4.5$. The dependence on the event generator is weak. Overall we estimate that the systematic error on the charge particle multiplicity is of the order of 5-8%.

Fig. 5 (left panel) shows the resulting pseudorapidity density distributions for six collision centralities for $65AGeV + 65AGeV$ Au+Au collisions. The stars denote independent estimates of the charged particle multiplicity obtained by counting tracks in the forward TPC of the midrapidity spectrometer. There is good consistency between the various independent measurements. From these distributions we can conclude that $dN(ch)/d\eta = 553 \pm 36$ for the most central collisions (0-5%). This number may also be compared to the PHOBOS result of 555 ± 35 [6] and the PHENIX result of $dN(ch)/d\eta = 609 \pm 37$ for 0-6% centrality cuts. Similar information for $100AGeV + 100AGeV$ Au+Au collisions is shown in fig. 5 (right panel). The corresponding numbers from BRAHMS [4] for the higher energy are $dN(ch)/d\eta = 632 \pm 36$, demonstrating an increase in multiplicity of about 14%.

By integrating the pseudorapidity distribution with respect to η we find that the

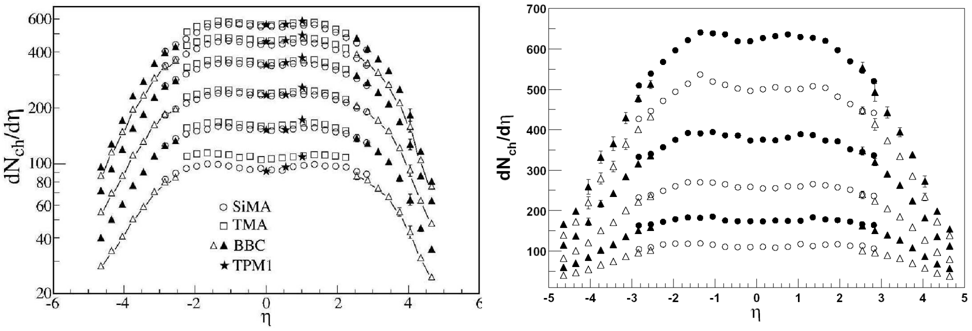

Figure 5. Distributions of $dN_{ch}/d\eta$ vs η for centrality ranges of, top to bottom, 0-5%, 5-10%, 10-20%, 20-30%, 30-40%, and 40-50% at $\sqrt{s_{NN}} = 130$ GeV (left panel) and at $\sqrt{s_{NN}} = 200$ GeV (right panel). Statistical uncertainties are shown where larger than the symbol size. The connecting lines and alternating open and closed symbols for the BBC data are to help distinguish points associated with different centrality ranges.

total production of charged particles in Au+Au collisions at $\sqrt{s_{NN}} = 130$ GeV is $N(ch) = 3860 \pm 300$ for the most central collisions (0-5%) in the pseudorapidity range $(-4.7 < \eta < +4.7)$. The number for central collisions indicates that, on the average, 23 particles are produced per pair of participant nucleons. The result can be compared to the 17 charged particles deduced by interpolating the results from p+p collisions to the present CM energy. At the full energy of the RHIC collider $\sqrt{s_{NN}} = 200$ GeV we expect 20 charged particles per p+p collision, i.e. an increase of about 18%. The first results from $\sqrt{s_{NN}} = 200$ GeV show that the total multiplicity in the $-4.7 < \eta < +4.7$ range is 4630 ± 330, i.e. an increase by about 20% over the lower energy.

In fig. 6 (left panel) we show the charged particle densities normalized to the number of participant pairs $N_{part}/2$ for the two RHIC energies. Data are plotted as a function of pseudorapidity and shifted by the beam rapidity. Data from 9.4% central Pb+Pb reactions at CERN-SPS are also shown. The figure illustrates that the particle production is practically identical at rapidities closer to the beam rapidity. This

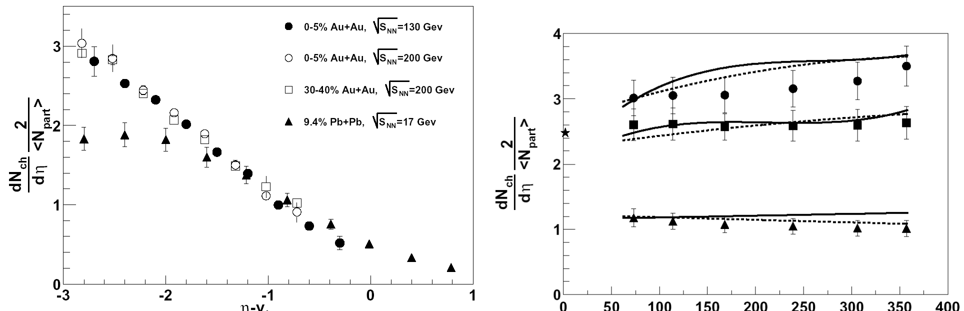

Figure 6. Left panel: Distribution of $dN_{ch}/d\eta$ divided by the number of pairs of participant baryons plotted as a function of pseudorapidity minus beam rapidity for BRAHMS data at $\sqrt{s_{NN}} = 130$, 200 GeV and SPS data. Right panel: Distribution of $dN_{ch}/d\eta$ divided by the number of pairs of participant baryons plotted as a function of number of participants for three pseudorapidity regions (top to bottom: $\eta = 0$, 3.0, 4.5) for for $\sqrt{s_{NN}} = 200$ GeV. AMPT calculations are shown with dashed lines; Kharzeev and Levin high density QCD predictions are shown with full lines.

supports the notion of a limiting behavior of particle production in the fragmentation region.

The systematics of the charged particle production per pair of participating baryons as a function of centrality for $\sqrt{s_{NN}}$ = 200 GeV is shown in fig. 6 (right panel). The data are compared to the AMPT model [7, 8, 9] and to the high density QCD model by Kharzeev and Levin [16]. The latter model is particularly interesting as it includes the effects of a saturation of the particle production due to a saturation in the number of gluon collisions. A good consistency between the data and the Kharzeev and Levin model is found. However, is should also be noted that AMPT reproduces the data almost as well.

5. Rapidity dependence of ratios of identified particles

BRAHMS has measured the K$^-$ to K$^+$ ratio at different rapidities for $\sqrt{s_{NN}}$ = 130 GeV reactions, the K$^-$ to K$^+$ ratios are 0.90 ± 0.06 ($y \approx 0$) and 0.83 ± 0.1 ($y \approx 2.5$). Preliminary results on the K to π ratios are shown in fig. 7 [15] (left panel) for $\sqrt{s_{NN}}$ = 130 GeV and 0-40% centrality. The ratios reach values of about 17% in the p_T range close to the mean transverse momenta of kaons and pions and increase with increasing p_T. In the right panel, the antiproton to proton and the K$^+$ to K$^-$ at $y \approx 0$ and at $y \approx 2.0 - 2.5$ are compared to a thermal model calculation [26].

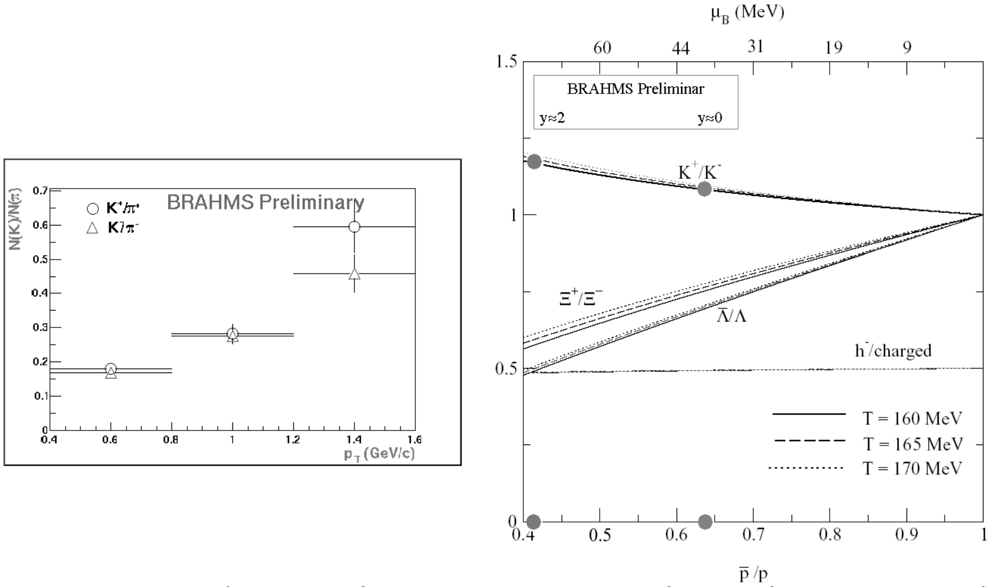

Figure 7. Left panel: K to π ratios as a function of p_T at midrapidity for $\sqrt{s_{NN}}$ = 130 GeV. Right panel: Comparison of antiparticle to particle ratios measured at midrapidity and at forward rapidity to a thermal model [26].

6. Summary

In summary, the BRAHMS experiment has measured the centrality dependence of the pseudorapidity distribution of charged particles and the ratio of positive and negative pions, kaons and protons at central and forward rapidities. The pion ratios are close to unity as would be expected at these energies, where about 4000−5000 charged particles (predominantly pions) are produced per central collision. The K^- to K^+ ratios are 0.90 ± 0.06 ($y \approx 0$) and 0.83 ± 0.1 ($y \approx 2.5$). As far as the baryons are concerned, we find that for central collisions at $\sqrt{s_{NN}} = 130$ GeV the ratio of antiprotons to protons is still significantly below unity at midrapidity and decreases towards forward rapidity.

7. Acknowledgements

This work was supported by the Division of Nuclear Physics of the Office of Science of the U.S. Department of Energy, the Danish Natural Science Research Council, the Norwegian Natural Science Research Council, the Polish Ministry of Research and the Korea Research Foundation Grant.

References

[1] I.G. Bearden *et al.* (BRAHMS collaboration), Nucl. Instrum. Meth., to be published; D. Beavis *et al.* (BRAHMS collaboration), *Conceptional Design Report for BRAHMS*, BNL-62018 (www.rhic.bnl.gov/brahms/WWW/cdr/cdr.html).
[2] C. Adler, A. Denisov, E. Garcia, M. Murray, H. Strobele, S. White, Nucl. Instrum. Meth. **A461** (2001) 337; nucl-ex/0008005.
[3] I. G. Bearden *et al.* (BRAHMS collaboration), Phys. Lett. **B253** (2001) 227.
[4] I. G. Bearden *et al.* (BRAHMS collaboration), submitted to Phys. Rev. Lett. (2001), nucl-ex. 00112001.
[5] I.G. Bearden *et al.* (BRAHMS collaboration), Phys. Rev. Lett. **87** (2001) 112305.
[6] B.Back *et al.* (PHOBOS collaboration), Phys. Rev. Lett. **85** (2000) 3100.
[7] Bin Zhang, C.M. Ko, Bao-An Li, and Ziwei Lin, Phys. Rev. **C61** (2001) 067901.
[8] Zi-wei Lin, Subrata Pal, C.M. Ko, Bao-An Li, and Bin Zhang, Phys. Rev. **C64** (2001) 011902(R).
[9] Zi-wei Lin, Subrata Pal, C.M. Ko, Bao-An Li, and Bin Zhang, preprint nucl-th/0105044; and Zi-wei Lin, private communication.
[10] L. Ahle *et al.* (E802 collaboration), Phys. Rev. Lett. **81** (1998) 2650.
[11] I. G. Bearden *et al.* (NA44 collaboration), J. Phys. G, Nucl. Part. **23** (1997) 1865.
[12] HIJING with Parton shadowing and Jet quench. X-N. Wang and M. Gyulassy, Phys. Rev. **D44** (1991) 3501.
[13] FRITIOF 7.02. H. Pi, Comp. Phys. Comm. 2000.
[14] S.A. Bass et al, Prog. Part. Nucl. Phys. **41** (1998) 225 and M. Bleicher et al. J. Phys. G. Nucl. Part. **25** (1999) 1859.
[15] J.H. Lee (BRAHMS collaboration), *Workshop on Thermalization and Chemical Equilibration in Heavy Ions Collisions at RHIC*, July 20-21, 2001, Brookhaven National Laboratory, Long Island, New York, USA.
[16] D. Kharzeev and E. Levin. nucl- th. 0108006, and private communication.
[17] G. Cooper *et al.* (NA49 Collaboration), Nucl. Phys. **A661** (1999) 362c.
[18] B. Back *et al.* (E917 Collaboration), Phys. Rev. Lett. **86** (2001) 1970.
[19] F. Videbaek and O. Hansen, Phys. Rev. **C52** (1995) 2684; F. Videbaek, nucl-ex/0106017.
[20] N. Herrmann, J.P. Wessels and T. Wienold, Ann. Rev. Nucl. Part. Sci. **49** (1999) 581.
[21] C. Adler *et al.* (STAR Collaboration), Phys. Rev. Lett. **86** (2001) 4778-4782.
[22] F. Videbaek *et al.* (BRAHMS Collaboration), *Results from first RHIC run*, Proc. Quark Matter 2001, Stony Brook, NY, USA, January 2001, to be published in Nucl. Phys. **A**.
[23] B. Jacak (PHENIX Collaboration), *Colloque International pour la Physique du Plasma Quark Gluon, CIPPPQG*, Ecole Polytechnique, Palaiseau, France, September 4-7, 2001, to be published.
[24] G. Veres *et al.* (NA49 Collaboration), Nucl. Phys. **A661** (1999) 383.
[25] I.G. Bearden *et al.* (BRAHMS Collaboration), Phys. Rev. Lett. **87** (2001) 112305.
[26] F. Becattini, J. Cleymans, A. Keränen, E. Suhonen, K. Redlich, Phys.Rev. **C64** (2001) 024901.